

Structure, Magnetism, and Multi-electron Reduction Reactivity of the Inverse Sandwich Reduced Arene La^{2+} Complex $[[\text{C}_5\text{H}_3(\text{SiMe}_3)_2]_2\text{La}]_2(\mu\text{-}\eta^6\text{-}\eta^6\text{-C}_6\text{H}_6)]^{1-}$

Chad T. Palumbo,[†] Lucy E. Darago,[‡] Megan T. Dumas,[†] Joseph W. Ziller,[†] Jeffrey R. Long,^{*,‡,§,||} and William J. Evans^{*,†}

[†]Department of Chemistry, University of California, Irvine, California 92697, United States

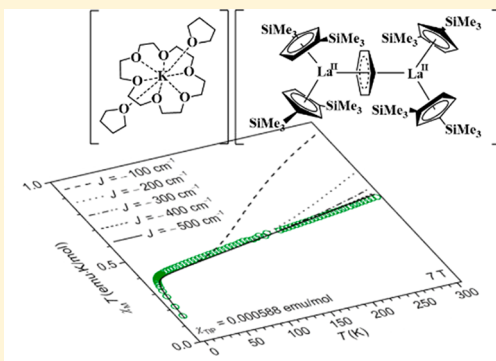
[‡]Department of Chemistry, University of California, Berkeley, California 94720, United States

[§]Materials Sciences Division, Lawrence Berkeley National Laboratory, Berkeley, California 94720, United States

^{||}Department of Chemical and Biomolecular Engineering, University of California, Berkeley, California 94720, United States

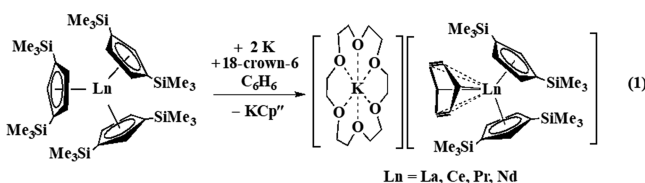
Supporting Information

ABSTRACT: The magnetic properties and multi-electron reductive reactivity of the bimetallic inverse sandwich La^{2+} complex salt, $[\text{K}(18\text{-crown-6})(\text{THF})_2][(\text{Cp}''\text{La})_2(\mu\text{-}\eta^6\text{-}\eta^6\text{-C}_6\text{H}_6)]\cdot\text{THF}$, **1** ($\text{Cp}'' = \text{C}_5\text{H}_3(\text{SiMe}_3)_2$), originally described by Lappert et al., have been examined. The compound was prepared by reduction of $\text{Cp}''_3\text{La}$ with potassium metal in benzene and crystallographically characterized. Compound **1** can be described as containing two Sd^1 $\text{La}(\text{II})$ ions bridged by a planar (C_6H_6)¹⁻ benzenide bridged radical monoanion, with fits to its variable-temperature magnetic susceptibility data revealing strong antiferromagnetic exchange coupling, with $J_{\text{La-C}_6\text{H}_6} > -400 \text{ cm}^{-1}$. The multi-electron reduction reactivity of **1** was explored in reactions with anthracene, naphthalene, and cyclooctatetraene. Compound **1** reduces anthracene to give $\text{Cp}''_2\text{La}(\mu\text{-}\eta^6\text{-}\eta^6\text{-C}_{14}\text{H}_{10})\text{K}(18\text{-crown-6})$, **2**, which contains a nonplanar anthracenide dianion with an end ring interacting with $\text{La}(\text{III})$ and the central ring interacting with potassium. The reaction of **1** with naphthalene forms $[\text{K}(18\text{-crown-6})(\text{THF})_2][\text{Cp}''_2\text{La}(\eta^4\text{-C}_{10}\text{H}_8)]$, **3**, which has a naphthalenide dianion with one planar ring and one ring bent such that four carbon atoms have $2.663(4)\text{--}2.743(4) \text{ \AA}$ La-C distances. 1,3,5,7-Cyclooctatetraene is reduced by **1** to give the bridged cyclooctatetraenyl complex salt $[\text{K}(18\text{-crown-6})][(\mu\text{-}\eta^8\text{-C}_8\text{H}_8)\text{LaCp}''(\mu\text{-}\eta^8\text{-C}_8\text{H}_8)\text{LaCp}''_2]$, **4**.



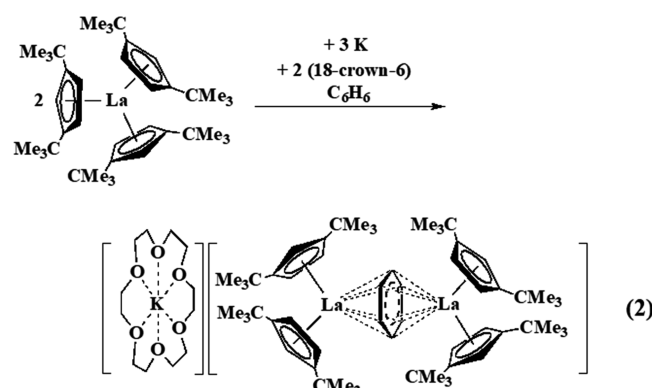
INTRODUCTION

Early studies in reductive rare-earth metal chemistry in the presence of arenes by Lappert and co-workers revealed a series of interesting $(\text{C}_5\text{R}_5)_3\text{Ln}/\text{K}$ reactions that gave products formulated to contain (arene)¹⁻ and (arene)²⁻ anions on the basis of X-ray crystallography.^{1–3} Equation 1 shows that reduction of the tris(cyclopentadienyl) complex, $\text{Cp}''_3\text{Ln}$ ($\text{Cp}'' = \text{C}_5\text{H}_3(\text{SiMe}_3)_2$), with excess K in the presence of 18-crown-6 forms a La^{3+} complex of a bent (C_6H_6)²⁻ dianion.¹



Equation 2 shows a variation of this reaction using 1.5 equiv of K metal per La, which is coordinated by the all-carbon analogue of the Cp'' ligand, namely, $\text{Cp}''^t = \text{C}_5\text{H}_3^t\text{Bu}_2$.² In this case, the reduction gave an inverse sandwich arene compound that was postulated to be a La^{2+} complex of a planar (C_6H_6)¹⁻ monoanion.

An analogous reaction with Cp'' was reported, but crystals suitable for X-ray diffraction were not obtained.²

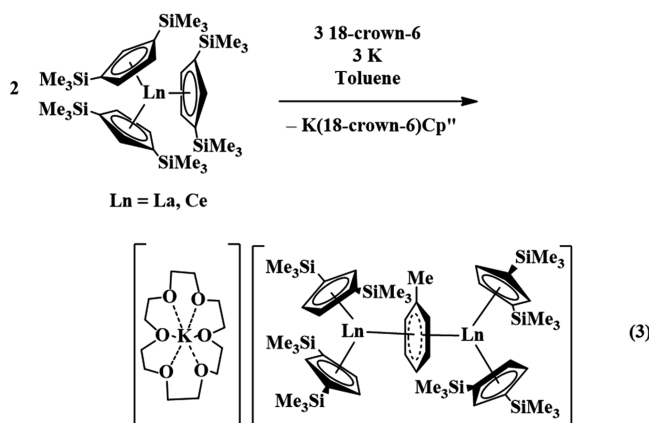


Reactions with the stoichiometry of eq 2 but with the silylcyclopentadienyl analogues, $\text{Cp}''_3\text{Ln}$ ($\text{Ln} = \text{La, Ce}$), and with toluene instead of benzene were also described (eq 3).³

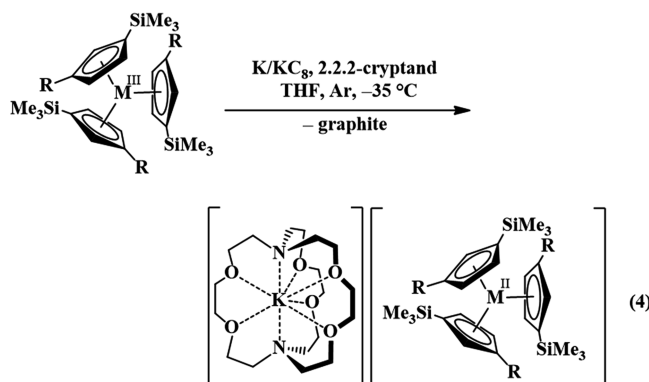
Received: July 24, 2018

Published: September 24, 2018

Although there was disorder in the crystal structure that limited the quality of the data, these inverse sandwich complexes were reported as Ln^{2+} complexes of planar $(\text{C}_6\text{H}_5\text{CH}_3)^{1-}$ monoanions derived from toluene.

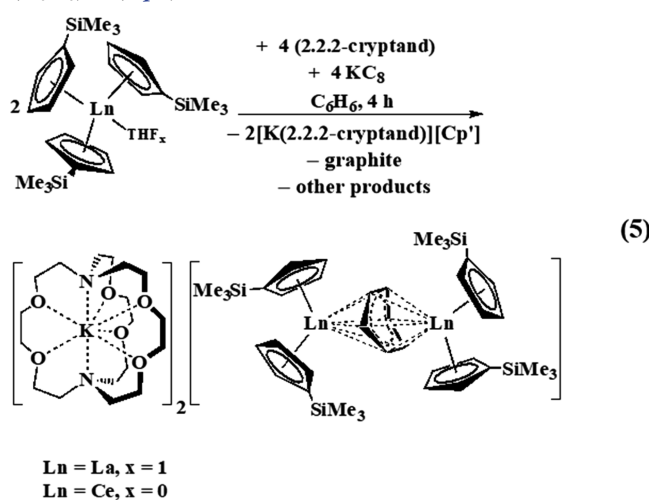


The known difficulty in assigning oxidation states in bridging arene systems along with the disorder in the crystal structures complicated the oxidation state assignments until unambiguous examples of complexes of La^{2+} were found, as shown in eq 4.^{4–13} Subsequently, Ln^{2+} complexes of all the lanthanides except radioactive promethium were isolated from $\text{Cp}'_3\text{Ln}$ precursors (eq 4).^{14–19}

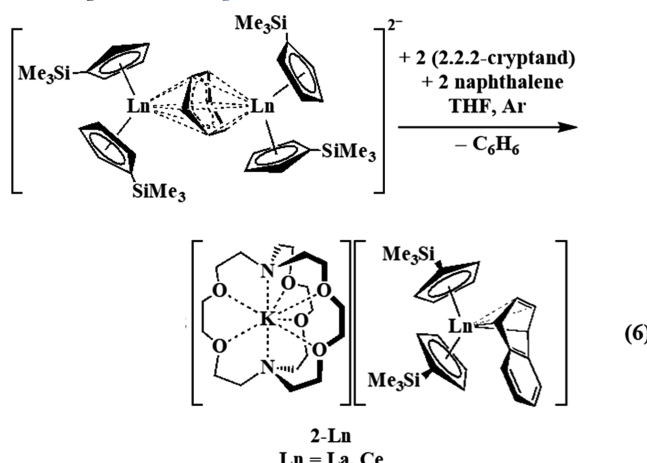


$\text{R} = \text{SiMe}_3$; $\text{M} = \text{La}$
 $\text{R} = \text{H}$; $\text{M} = \text{Y, La, Ce, Pr, Nd, Sm, Gd, Tb, Dy, Ho, Er, Tm, Lu}$

Further studies of reductions analogous to eqs 1 and 2 but with tris(monosilylcyclopentadienyl) lanthanide precursors gave Ln^{2+} inverse sandwich complexes of the benzene dianion, $(\text{C}_6\text{H}_6)^{2-}$ (eq 5).²⁰



These complexes were found to act as four-electron reductants with naphthalene (eq 6).²⁰



Our interest in multi-electron reduction chemistry stimulated us to ask if (arene) $^{1-}$ monoanion complexes of Ln^{2+} postulated in eqs 2 and 3 could also act as multi-electron reductants. These complexes could exhibit different reactivity from that in eq 6 since they are potentially three-electron reductants. In that regard, we focused on lanthanum as the metal, since La^{3+} is diamagnetic, and we focused on Cp'' as the ligand in order to make a Cp'' vs Cp' comparison with eq 6. We report here the successful crystallization of the Cp'' analogue of eq 2, namely, $[\text{K}(18\text{-crown-6})(\text{THF})_2][(\text{Cp}'_2\text{La})_2(\mu\text{-}\eta^6\text{:}\eta^6\text{-C}_6\text{H}_6)]$, 1, and its multi-electron reactivity with anthracene, naphthalene, and cyclooctatetraene.

Compound 1 is particularly unusual because of its apparent thermal stability: Lappert and co-workers reported that it could be made from the $[\text{K}(18\text{-crown-6})][\text{Cp}''_2\text{La}(\text{C}_6\text{H}_6)]$ product of eq 1 by heating this compound at 70°C for over 7 days. Furthermore, since 1 is a rare example of a complex containing two nontraditional ($4p^15d^1$) divalent lanthanide ions bridged by a radical ligand, its magnetic susceptibility was also studied. The magnetic exchange coupling behavior of 1 is of interest for comparison to that observed for bimetallic trivalent rare-earth metal complexes bridged by radical ligands.^{21–31}

EXPERIMENTAL DETAILS

The syntheses and manipulations described below were conducted under argon with rigorous exclusion of air and water using glovebox, vacuum line, and Schlenk techniques. Solvents were sparged with UHP grade argon (Praxair) and passed through columns containing Q-5 and molecular sieves before use. NMR solvents (Cambridge Isotope Laboratories) were dried over NaK /benzophenone, degassed by three freeze–pump–thaw cycles, and vacuum transferred prior to use. Anhydrous $\text{Cp}''_3\text{La}$ ³² was prepared according to the literature. 18-Crown-6 (1,4,7,10,13,16-hexaoxacyclooctadecane, Aldrich) was sublimed before use. ^1H NMR (500 MHz) and ^{13}C NMR (125 MHz) spectra were obtained on a Bruker GN500 or CRYO500 MHz spectrometer at 298 K. IR samples were prepared as KBr pellets, and the spectra were obtained on a Jasco FT/IR-4700 spectrometer. Elemental analyses were performed on a PerkinElmer 2400 Series II CHNS elemental analyzer. UV–vis spectra were collected in THF at 298 K using a Varian Cary 50 Scan UV–vis spectrophotometer.

[K(18-crown-6)(THF)₂][$(\text{Cp}''_2\text{La})_2(\mu\text{-}\eta^6\text{:}\eta^6\text{-C}_6\text{H}_6)]\text{-THF, 1}$. Compound 1 was prepared as an adaptation to the previously reported literature.² In a glovebox free of coordinating solvents, $\text{Cp}''_3\text{La}$ (373 mg,

0.486 mmol) and 18-crown-6 (193 mg, 0.729 mmol) were dissolved in C_6H_6 and then transferred to a vial containing potassium (29 mg, 0.729 mmol), and a slow color change to dark purple was observed. Over the course of 4 days, the solution turned to a dark slurry. Dark green solids were separated from the dark red supernatant and subsequently washed with benzene (2×5 mL). The resultant dark green solids were transferred to another glovebox and dissolved in THF (5 mL), which gave an intense blue solution. The dark blue THF solution was layered with Et_2O (15 mL) and stored at $-35^\circ C$ in the glovebox freezer for 4 days to yield dark green single crystals characterized by X-ray diffraction as **1** (246 mg, 61%). The 1H NMR and EPR spectra of **1** matched those previously reported.² IR: 3066w, 3053w, 2948s, 2890m, 1471w, 1453w, 1432w, 1398w, 1351m, 1314w, 1283w, 1246s, 1213w, 1107s, 1077s, 1056m, 961m, 923m, 828s, 770m, 749s, 683m, 638m, 625w, 601w cm^{-1} . UV-vis (THF) λ_{max} nm (ϵ , $M^{-1} cm^{-1}$): 268 (17200), 340 (1440), 410 (8300 shoulder), 583 (11900), 710 (6700). Anal. Calcd for $C_{74}H_{138}KLa_2O_9Si_8$: C, 51.87; H, 8.12. Found: C, 51.48; H, 7.89.

Cp''₂La(C₁₄H₁₀)K(18-crown-6), 2. In a glovebox, a scintillation vial was charged with compound **1** (40 mg, 28 μ mol) and THF (5 mL) to give an intensely colored ink-blue solution. The solution was stirred until compound **1** was fully dissolved, and then anthracene (5 mg, 28 μ mol) in THF (5 mL) was added and the mixture was left to stir for 1 h. After 1 h, the reaction mixture was heated with a hot plate set to $75^\circ C$ and left to stir again for 1 h, and the solution turned from dark blue to dark violet. The volatiles were removed *in vacuo*, and the resultant dark solids were extracted into toluene (10 mL). The green insoluble materials (presumably unreacted **1**, dissolution in THF gave a dark blue solution) were removed via centrifugation, and the toluene was removed from the supernatant *in vacuo*. The resultant solids were dissolved in Et_2O (8 mL), filtered, and concentrated before 5–8 drops of toluene were added. The solution was stored overnight at $-35^\circ C$ in the glovebox freezer to yield violet single crystals of $Cp''_2La(C_{14}H_{10})K(18\text{-crown-6})$, **2**, characterized by X-ray crystallography (11 mg, 38%). IR: 3075w, 3051w, 2953s, 2895m, 1451m, 1435m, 1425m, 1402m, 1385w, 1352m, 1315m, 1246s, 1211m, 1113m, 1078s, 1059m, 962m, 920s, 831s, 775s, 750s, 716w, 691m, 640m, 621m cm^{-1} . Anal. Calcd for $C_{48}H_{76}KLaO_6Si_4$: C, 55.46; H, 7.37. Numerous samples were examined that had low values suggesting incomplete sample combustion:^{4,33–37} C, 53.86; H, 6.92; C, 53.60; H, 7.04; C, 49.53; H, 6.62. The found CH ratios of $C_{48}H_{73.5}$, $C_{48}H_{75.1}$, and $C_{48}H_{76.4}$ are close with the calculated $C_{48}H_{76}$ formula.

[K(18-crown-6)(THF)₂][Cp''₂La(C₁₀H₈)], 3. In a glovebox, a scintillation vial was charged with compound **1** (25 mg, 18 μ mol) and THF (4 mL) to give an intensely colored ink-blue solution. The solution was stirred until compound **1** was fully dissolved, and then naphthalene (2 mg, 18 μ mol) in THF (4 mL) was added and the mixture was left to stir for 1 h. After 1 h, the reaction mixture was heated with a hot plate set to $75^\circ C$ and left to stir again for 1 h, and the solution turned from dark blue to dark green. The volatiles were removed *in vacuo*, and the resultant dark solids were extracted into toluene (10 mL). The green insolubles (presumably unreacted **1**, dissolution in THF gave a dark blue solution) were removed via centrifugation, and the toluene of the supernatant was removed *in vacuo*. The resultant solids were dissolved in a 4:1:1 Et_2O /THF/toluene solution (2 mL) and filtered. Dark green single crystals characterized by X-ray crystallography as $[K(18\text{-crown-6})(THF)_2][Cp''_2La(C_{10}H_8)]$, **3**, were obtained by vapor diffusion of pentane into the dark green solution at $-35^\circ C$ (7 mg, 35%). IR: 3069w, 3038w, 2951s, 2897s, 1476m, 1452m, 1437m, 1400m, 1385m, 1352s, 1315w, 1285w, 1265m, 1248s, 1215w, 1184w, 1111s, 1078s, 1057w, 1005w, 999w, 962m, 924m, 833s, 787w, 773w, 750m, 731w, 692w, 685w, 640w cm^{-1} . Anal. Calcd for $C_{52}H_{90}KLaO_8Si_4$: C, 55.09; H, 8.00. Found: C, 50.51; H, 7.14. The found CH ratio of $C_{48}H_{86.4}$ is consistent with the formula and suggests incomplete combustion.^{4,33–37}

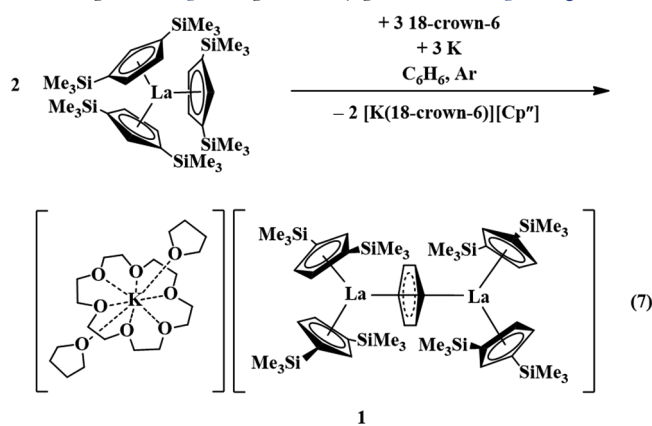
[K(18-crown-6)][(C₈H₈)LaCp''(C₈H₈)LaCp''₂], 4. In a glovebox, a scintillation vial was charged with **1** (166 mg, 0.1 mmol) and THF (12 mL) to give an intensely colored ink-blue solution. C_8H_8 (15 mg, 0.15 mmol) dissolved in THF (6 mL) was added to the stirred solution, and the mixture immediately turned bright yellow. After 1 h, the

volatiles were removed to yield yellow solids. Et_2O was added (15 mL) and the yellow slurry was filtered and concentrated to ca. 3 mL. The yellow solution was then layered with hexane (15 mL) and stored at $-35^\circ C$ in the glovebox freezer to yield yellow single crystals (40 mg, 29%) characterized by X-ray crystallography as $[K(18\text{-crown-6})][(C_8H_8)LaCp''(C_8H_8)LaCp''_2]$, **4**. 1H NMR (THF- d_8): δ 7.18 (t, $^3J_{HH} = 9$ Hz, 2H, $\{[C_5H_3(SiMe_3)_2]_2La\}$), 7.09 (d, $^3J_{HH} = 9$ Hz, 1H, $\{[C_5H_3(SiMe_3)_2]_2La\}$), 6.74 (d, $^3J_{HH} = 6$ Hz, 1H, $\{[C_5H_3(SiMe_3)_2]_2La\}$), 6.69 (br s, 2H, $\{[C_5H_3(SiMe_3)_2]_2La\}$), 6.31 (d, $^3J_{HH} = 12$ Hz, 8H, C_8H_8), 6.24 (br s, 8H, C_8H_8), 3.17 (br s, 24H, $[K(18\text{-crown-6})]$), 0.48 (br s, 36H, $\{[C_5H_3(SiMe_3)_2]_2La\}$), 0.46 (s, 18H, $\{[C_5H_3(SiMe_3)_2]_2La\}$). $^{13}C\{^1H\}$ NMR (THF- d_8): δ 136.53 $\{[C_5H_3(SiMe_3)_2]_2La\}$, 132.21 $\{[C_5H_3(SiMe_3)_2]_2La\}$, 129.49 $\{[C_5H_3(SiMe_3)_2]_2La\}$, 128.72 $\{[C_5H_3(SiMe_3)_2]_2La\}$, 128.54 $\{[C_5H_3(SiMe_3)_2]_2La\}$, 125.87 $\{[C_5H_3(SiMe_3)_2]_2La\}$, 98.27 (C_8H_8), 94.54 (C_8H_8), 70.24 $[K(18\text{-crown-6})]$), 1.94 $\{[C_5H_3(SiMe_3)_2]_2La\}$, 1.82 $\{[C_5H_3(SiMe_3)_2]_2La\}$. FT-IR: 2949s, 2890s, 2859m, 2826m, 2796w, 2750w, 2709w, 1980w, 1958w, 1930w, 1868w, 1832w, 1720w, 1571w, 1472m, 1453m, 1437m, 1399w, 1351s, 1319w, 1283w, 1252s, 1229m, 1113s, 1079s, 965s, 919m, 894w, 830s, 751s, 703s, 693s, 631m, 623m cm^{-1} . Anal. Calcd for $C_{61}H_{99}K_1La_2O_6Si_6$: C, 51.82; H, 7.06. Found: C, 51.59; H, 7.34.

Magnetic Measurements. Samples were prepared by adding the crystalline compound to a 5 mm inner diameter quartz tube containing a raised quartz platform. Compound **1** was measured under both unground and ground (ground for 15 min using an agate mortar and pestle) conditions. For all samples, solid eicosane was added to prevent crystallite torquing and to provide good thermal contact between the sample and the bath. The tubes were fitted with Teflon sealable adapters, evacuated using a glovebox vacuum pump, and flame-sealed under static vacuum. Following flame sealing, the solid eicosane was melted in a water bath held at $40^\circ C$. Magnetic susceptibility measurements were performed using a Quantum Design MPMS2 SQUID magnetometer. Dc magnetic susceptibility data were collected at temperatures ranging from 2 to 300 K, using applied magnetic fields of 0.1, 1, and 7 T. Diamagnetic corrections were applied to the data using Pascal's constants to give $\chi_D = -0.00104674$ emu/mol (**1**) and $\chi_D = -0.00024036$ emu/mol (eicosane).³⁸ Magnetic data modeling was performed using the program PHI.³⁹

RESULTS

Synthesis and Crystallographic Characterization of $[K(18\text{-crown-6})(THF)_2][(Cp''_2La)_2(\mu-\eta^6:\eta^6-C_6H_6)]\cdot THF$, **1.** The reduction of Cp''_3La with 1.5 equiv of K metal with equimolar amounts of 18-crown-6 in benzene was repeated as originally reported by Lappert et al.² in the paper that described the structure of the Cp''_3La complex in eq 2. A dark green product was obtained, as reported. Dark green crystals of **1** could be obtained upon diffusion of Et_2O into an intense ink-blue THF solution generated after dissolution of the green solids. The UV–visible spectrum of a 0.75 mM solution of **1** in THF is shown in Figure 1. X-ray crystallography revealed that this was the Cp'' analogue of the complex in eq 2, as previously postulated (eq 7, Figure 2).



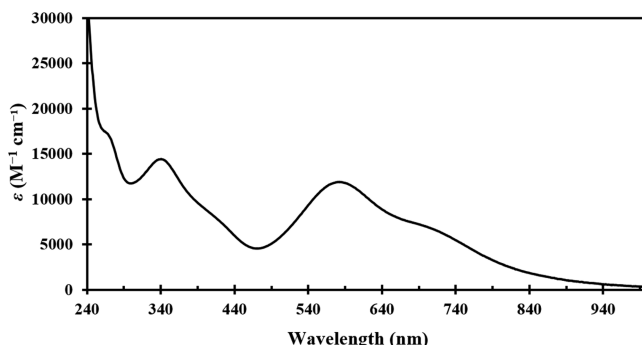


Figure 1. UV-visible spectrum of a 0.75 mM solution of $[\text{K}(18\text{-crown-6})(\text{THF})_2][(\text{Cp}''_2\text{La})_2(\mu\text{-}\eta^6\text{:}\eta^6\text{-C}_6\text{H}_6)]\cdot\text{THF}$, **1**, in THF at 298 K.

Compound **1** crystallizes in the *Pnma* space group, and the centrosymmetric anion can be described as two $\text{Cp}''_2\text{La}(\text{II})$ metallocene units bridged by a monoanionic arene ligand. There is disorder in the cyclopentadienyl rings in the crystal, such that this is a “connectivity only” structure. The overall structure exhibits a rectangular array of Cp'' ring centroids and a planar bridging arene anion (see Figures S1 and S2 in the SI).

Magnetic Susceptibility. Magnetic susceptibility times temperature ($\chi_M T$) versus temperature data for **1** were collected under applied magnetic fields of 0.1, 1, and 7 T (Figure S3). The $\chi_M T$ product of **1** exhibits a linear increase with increasing temperature due to temperature-independent paramagnetism, in which low-lying magnetic excited states become thermally populated at higher temperatures, a behavior that dominates under all of the applied magnetic fields probed. The temperature-independent paramagnetism likely stems from low-lying excited f^1 states on the La^{2+} ions, or possibly excited $5d$ states that have some orbital angular momentum. Under an applied field of 7 T, the $\chi_M T$ product at 300 K is 0.537 emu·K/mol,

approaching that expected for an antiferromagnetically coupled spin-only $S = 1/2$ system, 0.375 emu·K/mol, and substantially lower than the 1.125 emu·K/mol expected for three magnetically isolated $S = 1/2$ centers.

The linear temperature dependence of $\chi_M T$ at 7 T above 20 K suggests that temperature-independent paramagnetism behavior persists even under this strong magnetic field. The data can be modeled assuming a spin-only $S = 1/2$ system, with a χ_{TIP} of 0.000588 emu·K/mol (Figure S4). Since magnetic data for **1** can be treated assuming an antiferromagnetically coupled $S = 1/2$ system which persists even at room-temperature, the magnitude of the magnetic coupling between the $5d^1 \text{La}^{2+}$ spins and the radical $S = 1/2$ spin on the $(\text{C}_6\text{H}_6)^{1-}$ ligand must be quite large. Indeed, use of the spin-only Hamiltonian

$$\hat{H} = -2(J_{\text{La}-\text{C}_6\text{H}_6})(\hat{S}_{\text{C}_6\text{H}_6} \cdot (\hat{S}_{\text{La}(1)} + \hat{S}_{\text{La}(2)})) + \sum_{i=\text{La}, \text{C}_6\text{H}_6} \mu_B \hat{S}_{\text{g}_i} H \quad (8)$$

to model $\text{La}^{2+}-(\text{C}_6\text{H}_6)^{1-}$ exchange coupling, $J_{\text{La}-\text{C}_6\text{H}_6}$, along with a χ_{TIP} of 0.000588 emu·K/mol suggests that magnetic exchange must be stronger than -400 cm^{-1} (Figure 3). This is consistent with the degree of magnetic exchange observed in the similar complex $[\text{K}(2.2.2\text{-cryptand})_2][(\text{Cp}'_2\text{La})_2(\mu\text{-}\eta^6\text{:}\eta^6\text{-C}_6\text{H}_6)]$, which contains two $d^1 \text{La}^{2+}$ bridged through an $S = 1$ $(\text{C}_6\text{H}_6)^{2-}$ ligand.²⁰ In $[\text{K}(2.2.2\text{-cryptand})_2][(\text{Cp}'_2\text{La})_2(\mu\text{-}\eta^6\text{:}\eta^6\text{-C}_6\text{H}_6)]$, the spins cancel such that the complex appears diamagnetic, with $J_{\text{La}-\text{C}_6\text{H}_6}$ estimated to be around -500 cm^{-1} , and with the results of DFT calculations indicating that the two highest occupied molecular orbitals exhibit extensive mixing between metal and π^* orbitals of the C_6H_6 ligand. Presumably, similar mixing occurs in complex **1**. These exchange coupling values are by far the largest yet observed for lanthanide ions, rivaled only by the $J_{\text{Gd}-\text{e}^-}$ of $+175(10) \text{ cm}^{-1}$ determined for

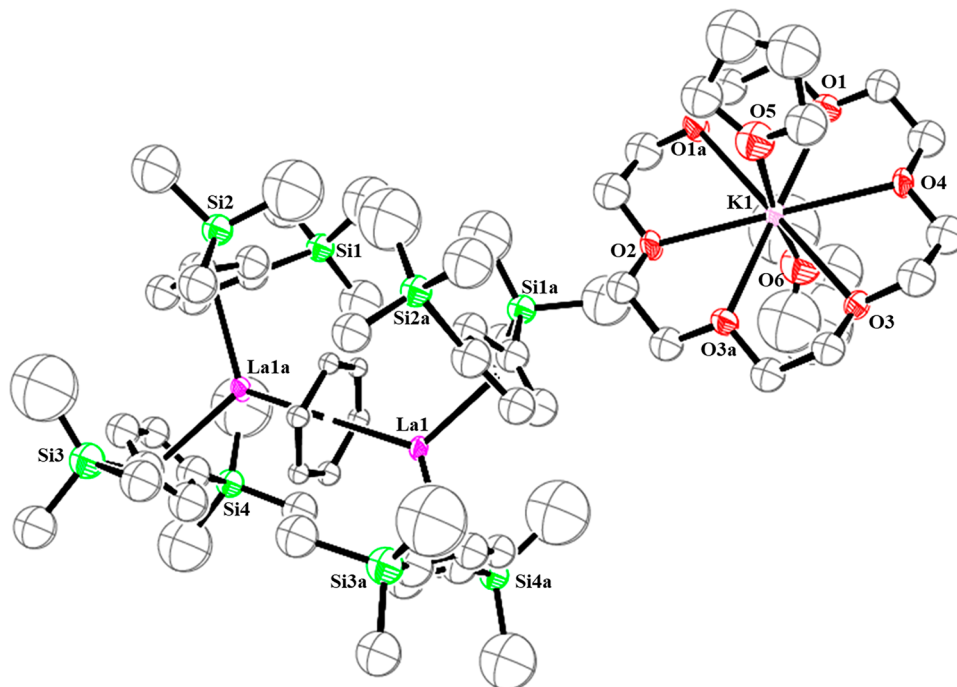


Figure 2. Molecular structure of $[\text{K}(18\text{-crown-6})(\text{THF})_2][(\text{Cp}''_2\text{La})_2(\mu\text{-}\eta^6\text{:}\eta^6\text{-C}_6\text{H}_6)]$, **1**, with thermal ellipsoids drawn at the 30% probability level. Hydrogen atoms and disorder of the silicon atoms are omitted for clarity. The silicon atoms are disordered between two positions with 50% occupancy (see SI).

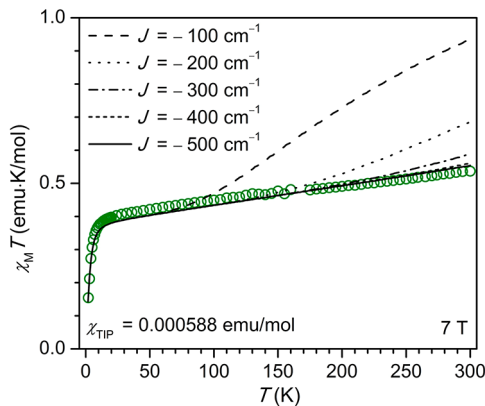


Figure 3. Plot of $\chi_M T$ versus temperature data for a ground sample of **1** collected under an applied magnetic field of 7 T, with models using eq 8 and different La^{2+} -radical coupling constants, J , shown by lines. Noise in data in the range 150–170 K is due to a crossover in the sign of the raw magnetic moment from negative to positive across these temperatures, during which the magnitude of the magnetic moment approached the sensitivity limit of the SQUID magnetometer. At some temperatures within this regime, clearly anomalous data points were removed entirely.

coupling between two Gd^{3+} ions and an electron “trapped” in a metal–metal bonding-type orbital in the endohedral metallofullerene complex $\text{Gd}_2@\text{C}_{79}\text{N}$.⁴⁰

The saturation magnetization of **1** at 2 K and 7 T also agrees with a ground state $S = 1/2$ assignment, with an experimental value of $1.02 \mu_B$ observed compared to the expected value of $1 \mu_B$ (Figure 4). Interestingly, in an unground sample of **1**, large

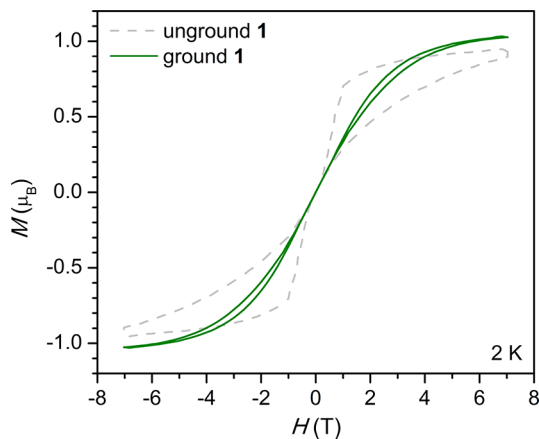


Figure 4. Magnetization (M) versus applied magnetic field (H) data for **1** at 2 K, where data for an unground sample of **1** are shown by the light gray dashed line, and data for a ground sample of **1** are shown by the solid green line. A magnetic field sweep rate of 0.4 mT s^{-1} was used.

magnetic hysteresis is observed at nonzero magnetic fields. In a ground sample of **1**, the degree of hysteresis is dramatically reduced, leading to the assignment of this field-induced slow-magnetic relaxation to a direct magnetic relaxation process affected by a spin-phonon bottleneck. A spin-phonon bottleneck is a phenomenon in which limited exchange between the spins and the thermal bath, which is mediated by low-energy phonons, slows down magnetic relaxation as a result of limited phonon density of states at low energy.^{41,42} This effect is most commonly observed in $S = 1/2$ systems in which magnetic relaxation occurs through the direct relaxation process, and has previously been

correlated with extrinsic sample characteristics, such as crystallite size.⁴³

Reactivity Studies. Anthracene. Addition of anthracene (reduction potential -1.74 V vs SHE)²⁴ to a dark blue solution of **1** in THF caused no color change. After the reaction was heated to 75°C for 1 h, the color changed to dark violet and the anthracenide complex salt, $\text{Cp}''_2\text{La}(\mu\text{-}\eta^6\text{-}\eta^4\text{-C}_{14}\text{H}_{10})\text{K}(18\text{-crown-6})$, **2**, was isolated in 38% yield and identified by X-ray crystallography (eq 9, Figure 5).

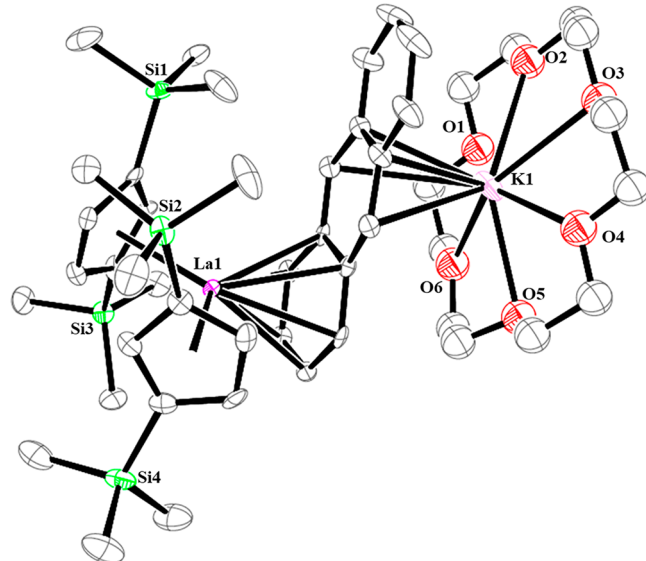
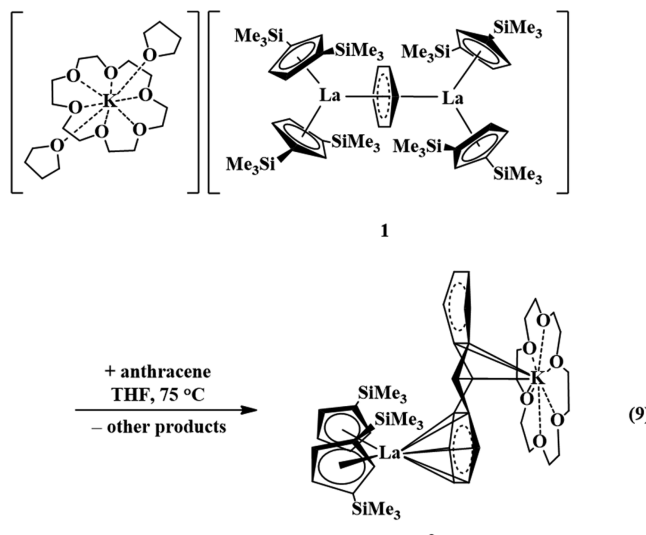


Figure 5. Thermal ellipsoid plot of $\text{Cp}''_2\text{La}(\mu\text{-}\eta^6\text{-}\eta^4\text{-C}_{14}\text{H}_{10})\text{K}(18\text{-crown-6})$, **2**, with thermal ellipsoids drawn at the 50% probability level. Hydrogen atoms and the disorder of 18-crown-6 are omitted for clarity. The 18-crown-6 is disordered between two positions at 50% occupancy (see SI).



In complex **2**, a $(\text{Cp}''_2\text{La})^+$ unit is bound to an end ring of anthracene and the $[\text{K}(18\text{-crown-6})]^+$ component is bound to the middle ring. The 18-crown-6 ring is disordered over at least two positions, and the data are not of sufficient quality to discuss bond distances. Previous studies have identified anthracenide dianion complexes of rare-earth metals. The ferrocene diamide complexes, $[\text{Fe}(\text{C}_5\text{H}_4^{\text{TBSN}})_2\text{Ln}(\text{THF})]_2(\mu\text{-}\eta^4\text{-}\eta^4\text{-C}_{14}\text{H}_{10})$ ($\text{Ln} = \text{Sc}$,⁴⁴ Y ;⁴⁵ $\text{TBSN} = \text{N}(\text{SiMe}_2\text{Bu})_2$), in the solid state have an

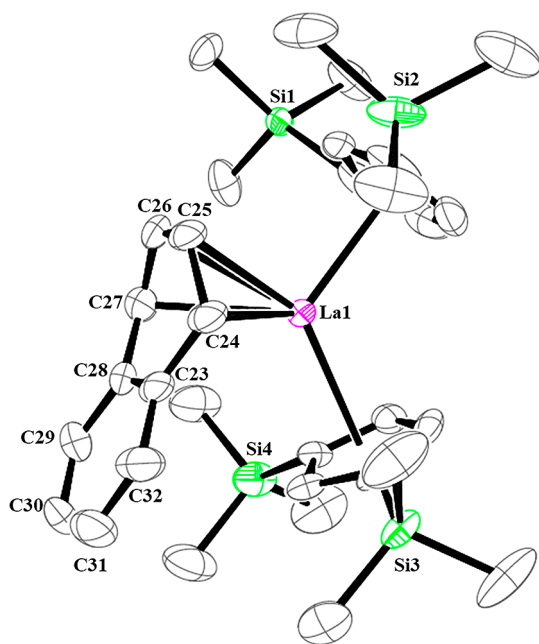
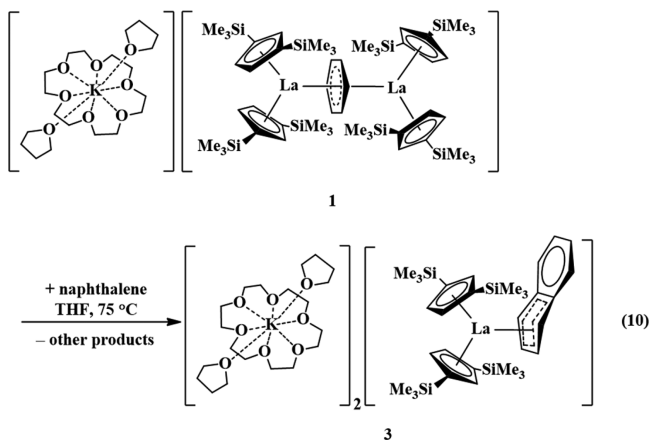


Figure 6. Thermal ellipsoid plot of $[K(18\text{-crown}\text{-}6)(\text{THF})_2][\text{Cp}''_2\text{La}(\eta^4\text{-C}_{10}\text{H}_8)]$, 3, with thermal ellipsoids drawn at the 50% probability level. Hydrogen atoms, the $[\text{K}(18\text{-crown}\text{-}6)(\text{THF})_2]^+$ cation, and disorder of the silicon atoms are omitted for clarity.

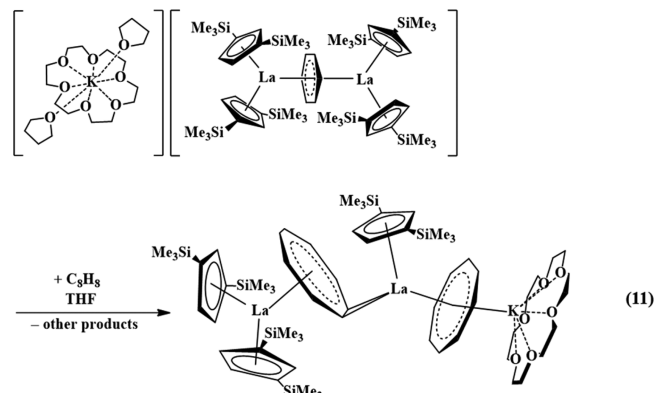
anthracene dianion moiety bent at the two central ring carbons (with torsion angles of 32.9° for Sc and 28.6° for Y) with one metal bound η^4 to the center ring carbon atoms and the other bound η^4 to the carbon atoms of a terminal ring. $[\text{K}(18\text{-crown}\text{-}6)][\text{Fe}(\text{C}_5\text{H}_4\text{TBsN})_2\text{Y}(\text{C}_{14}\text{H}_{10})]$ ⁸ is similar to the aforementioned complexes (with a torsion angle for the center ring of 33.9°), but it has a $[\text{K}(18\text{-crown}\text{-}6)]^+$ cation interacting with the terminal ring instead of Sc^{3+} or Y^{3+} . The bimetallic Y^{3+} amido phosphine, $[(\text{P}_2\text{N}_2)\text{Y}]_2(\text{C}_{14}\text{H}_{10})$ ($\text{P}_2\text{N}_2 = \text{PhP}(\text{CH}_2\text{SiMe}_2\text{NSiMe}_2\text{CH}_2)_2\text{PPh}_3$),⁴⁶ is similar to the previous complex and has η^4 coordination modes at the center and terminal rings, but a less distorted ring (with a torsion angle of 19.0°).

Naphthalene. No color change was observed upon addition of naphthalene (-2.36 V vs SHE)²⁴ to a dark blue solution of 1 in THF. However, heating the mixture to 75 °C for 1 h generated a green solution, from which crystals of $[\text{K}(18\text{-crown}\text{-}6)(\text{THF})_2][\text{Cp}''_2\text{La}(\eta^4\text{-C}_{10}\text{H}_8)]$, 3, could be isolated in 35% yield (eq 10, Figure 6). Complex 3 is the Cp'' 18-crown-6 analogue of the previously reported compound $[\text{K}(2.2.2\text{-cryptand})][\text{Cp}''_2\text{La}(\eta^4\text{-C}_{10}\text{H}_8)]$ ⁴⁷ shown in eq 6.



The bond distances and angles of 3 are presented along with the analogous values for $[\text{K}(2.2.2\text{-cryptand})][\text{Cp}''_2\text{La}(\eta^4\text{-C}_{10}\text{H}_8)]$ ⁴⁷ in Table 1. Both complexes feature a $(\text{Cp}''_2\text{La})^+$ metallocene unit oriented toward four carbon atoms of one ring of the $(\text{C}_{10}\text{H}_8)^{2-}$ ligand. The four carbon atoms are not coplanar with the remaining six carbon atoms. The angle between the two planes generated from (C24–C27) and (C23, C24, C27, C28) in 3 is 152.6° , which is similar to the 155.5° angle in $[\text{K}(2.2.2\text{-cryptand})][\text{Cp}''_2\text{La}(\eta^4\text{-C}_{10}\text{H}_8)]$. The 2.263 Å La–Mid1 distance defined by the midpoint of the vector between C24 and C27 in 3 is slightly longer than the analogous 2.230 Å distance in $[\text{K}(2.2.2\text{-cryptand})][\text{Cp}''_2\text{La}(\eta^4\text{-C}_{10}\text{H}_8)]$. The La–Cnt(Cp) distances of 3 are also slightly larger. In 3, they are 2.619 and 2.646 Å, and in $[\text{K}(2.2.2\text{-cryptand})][\text{Cp}''_2\text{La}(\eta^4\text{-C}_{10}\text{H}_8)]$, they are 2.610 and 2.592 Å. The 152.6° and 155.5° Cnt(Cp)–La–Cnt(Cp) angles are similar. These metrics suggest that the Cp'' coordination environment is comparable to Cp' in the $[\text{K}(\text{chelate})][\text{Cp}''_2\text{Ln}(\eta^4\text{-C}_{10}\text{H}_8)]$ complexes.

Cyclooctatetraene Reduction. The reaction of 1 with 1,3,5,7-cyclooctatetraene (-1.59 V vs SHE)²⁴ was also examined. In contrast to the above reactions, addition of C_8H_8 to 1 in THF caused an immediate color change to bright yellow without heating. Upon workup, yellow crystals of $[\text{K}(18\text{-crown}\text{-}6)][(\mu\text{-}\eta^8\text{-}\eta^2\text{-C}_8\text{H}_8)\text{LaCp}''(\mu\text{-}\eta^8\text{-}\eta^8\text{-C}_8\text{H}_8)\text{LaCp}''_2]$, 4, were isolated (eq 11, Figure 7).



Compound 4 crystallizes in the $Pna2_1$ space group and consists of an anionic component, $[\text{Cp}''_2\text{La}(\text{C}_8\text{H}_8)]^{1-}$, that appears similar to the anion $[\text{Cp}''_2\text{La}(\text{C}_8\text{H}_8)]^{1-}$ in crystals of the previously published compound $[\text{K}(2.2.2\text{-cryptand})][\text{Cp}''_2\text{La}(\eta^8\text{-C}_8\text{H}_8)]$,⁴⁸ but with Cp'' instead of Cp' and a $[\text{Cp}''\text{La}(\text{C}_8\text{H}_8)\text{K}(18\text{-crown}\text{-}6)]^+$ cation instead of $[\text{K}(2.2.2\text{-cryptand})]^+$. The metrical data for 4 are compared to $[\text{K}(2.2.2\text{-cryptand})][\text{Cp}''_2\text{La}(\eta^8\text{-C}_8\text{H}_8)]$ ⁴⁸ in Table 2. The $[\text{Cp}''_2\text{La}(\text{C}_8\text{H}_8)]^{1-}$ anion in 4 appears to be interacting with the $[\text{Cp}''\text{La}(\text{C}_8\text{H}_8)\text{K}(18\text{-crown}\text{-}6)]^+$ cation via an η^2 interaction of La2 with the $(\text{C}_8\text{H}_8)^{2-}$ ring bound η^8 to La1. This does not appear to have a substantial effect on the $[\text{Cp}''_2\text{La}(\text{C}_8\text{H}_8)]^{1-}$ unit, however. The 2.687 and 2.704 Å La1–Cnt(Cp') distances in 4 are similar to the 2.693 and 2.687 Å La1–Cnt(Cp') distances in $[\text{K}(2.2.2\text{-cryptand})][\text{Cp}''_2\text{La}(\eta^8\text{-C}_8\text{H}_8)]$,⁴⁸ despite the larger Cp'' ligand in 4. The La–Cnt(C₈H₈) distances are also similar; the 2.190 Å La1–Cnt(C₈H₈) distance in 4 is only 0.031 Å longer than the 2.159 Å distance in $[\text{K}(2.2.2\text{-cryptand})][\text{Cp}''_2\text{La}(\eta^8\text{-C}_8\text{H}_8)]$.⁴⁸ The 109.3° Cnt(Cp')–La1–Cnt(Cp') angle of 4 is only slightly larger than the analogous 107.1° angle in $[\text{K}(2.2.2\text{-cryptand})][\text{Cp}''_2\text{La}(\eta^8\text{-C}_8\text{H}_8)]$,⁴⁸ both of which are more acute than the 123.8° angle of the cationic

Table 1. Selected Bond Distances (Å) and Angles (deg) for $[\text{K}(18\text{-crown-6})(\text{THF})_2][\text{Cp}''\text{La}(\eta^4\text{-C}_{10}\text{H}_8)]$, 3, and $[\text{K}(2.2.2\text{-cryptand})][\text{Cp}''\text{La}(\eta^4\text{-C}_{10}\text{H}_8)]$ ^{47c}

| | 3 | $[\text{K}(2.2.2\text{-cryptand})][\text{Cp}''\text{La}(\eta^4\text{-C}_{10}\text{H}_8)]$ ^{47c} |
|--------------------------|----------|----------------------------------------------------------------------------------------------------------|
| Ln1–Cnt(Cp) | 2.619 | 2.592 |
| | 2.646 | 2.610 |
| Ln1–Mid1 ^a | 2.263 | 2.230 |
| Ln1–C(Cp) _{avg} | 2.89(2) | 2.865(7) |
| Ln1–C27 | 2.663(4) | 2.570(5) |
| Ln1–C24 | 2.694(4) | 2.689(3) |
| Ln1–C26 | 2.727(4) | 2.732(5) |
| Ln1–C25 | 2.743(4) | 2.772(6) |
| Ln1–C28 | 3.105(4) | 3.052(3) |
| Ln1–C23 | 3.134(4) | 3.068(3) |
| Cnt(Cp)–Ln1–Cnt(Cp) | 115.9 | 117.3 |
| Pln1–Pln2 ^b | 152.6 | 155.5 |

^aMid1 is the midpoint of the vector between C24 and C27. ^bPln1 and Pln2 are the planes of (C24–C27) and (C23–C24, C27–C28), respectively. ^cThe atom numbering is that of 3 with analogous distances shown for $[\text{K}(2.2.2\text{-cryptand})][\text{Cp}''\text{La}(\eta^4\text{-C}_{10}\text{H}_8)]$.⁴⁷

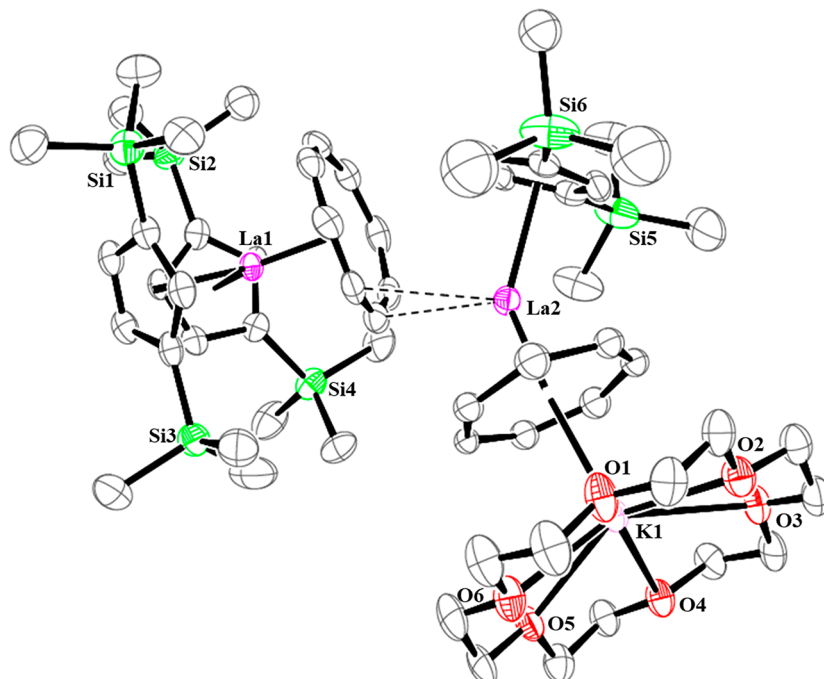


Figure 7. Thermal ellipsoid plot of $[\text{K}(18\text{-crown-6})][(\mu\text{-}\eta^8\text{:}\eta^2\text{-C}_8\text{H}_8)\text{LaCp}''(\mu\text{-}\eta^8\text{:}\eta^8\text{-C}_8\text{H}_8)\text{LaCp}'']$, 4, with thermal ellipsoids drawn at the 50% probability level. Hydrogen atoms, disorder of the methyl groups bound to Si1, and disorder of the $(\text{C}_8\text{H}_8)^{2-}$ ligands are omitted for clarity. The carbon atoms of the $(\text{C}_8\text{H}_8)^{2-}$ ligands bound to La2 were best refined with 57% occupancy over each of 14 disordered sites.

$[\text{Cp}''\text{La}(\text{DME})(\text{NC}^t\text{Bu})][\text{BPh}_4]$,⁴⁹ the 133.2° of $(\text{C}_5\text{Me}_5)_2\text{La}[\text{N}(\text{SiMe}_3)_2]$,⁵⁰ and the 131.6° angle in $(\text{C}_5\text{Me}_5)_2\text{La}(\text{BPh}_4)$.⁵¹ The $[\text{Cp}''\text{La}(\text{C}_8\text{H}_8)\text{K}(18\text{-crown-6})]^+$ cation in 4 consists of an inverse sandwich of a disordered $(\text{C}_8\text{H}_8)^{2-}$ ligand between $[\text{Cp}''\text{La}]^{2+}$ and $[\text{K}(18\text{-crown-6})]^+$ moieties. The 2.547 Å La2–Cnt(Cp) distance in the cation with one cyclopentadienyl ligand is significantly shorter than the 2.687 and 2.704 Å La1–Cnt(Cp) distances of the anion with two. The disorder in the $(\text{C}_8\text{H}_8)^{2-}$ prevents further discussion of the metrical parameters.

DISCUSSION

The crystallographic characterization of $[\text{K}(18\text{-crown-6})(\text{THF})_2][(\text{Cp}''\text{La})_2(\mu\text{-}\eta^6\text{:}\eta^6\text{-C}_6\text{H}_6)]$, 1, confirms the identity of the dark green powder first described by Lappert² as the bimetallic La(II) complex bridged by a benzenide monoanion

ligand, $(\text{C}_6\text{H}_6)^{1-}$. The structure of 1 is similar to the Cp^t analogue shown in eq 2 in that the four cyclopentadienyl ring centroids define a rectangle, not a tetrahedron, and the $(\text{C}_6\text{H}_6)^{1-}$ ligand is also planar. Also like the Cp^t analogue, the structure is highly disordered, limiting an analysis of the metrical parameters.

Complex 1 was of interest magnetically because it contains two nontraditional 4fⁿSd¹ Ln³⁺ ions, which, via their populated Sd orbitals, may engage in stronger magnetic exchange than the 4f orbitals of the Ln³⁺ ions.⁵² Previously, the Ln³⁺ complexes $\{[(\text{Me}_3\text{Si})_2\text{N}](\text{THF})\text{Ln}\}_2(\mu\text{-}\eta^2\text{:}\eta^2\text{-N}_2)\}[\text{K}(\text{L})]$ [Ln = Y, Gd, Tb, Dy, Ho, Er, Lu; L = 18-crown-6 or $(\text{THF})_6$] containing a radical N₂³⁻ bridge were obtained as products from LnA₃/M reductions.^{29,53,54} Magnetometry measurements revealed that the N₂³⁻ ligand provokes strong exchange coupling with the Ln³⁺ ions ($J_{\text{Gd}-\text{rad}} = -27$ cm⁻¹) which, when combined with the

Table 2. Selected Bond Lengths (Å) and Angles (deg) of $[K(18\text{-crown}\text{-}6)][(\mu\text{-}\eta^8\text{:}\eta^2\text{-}C_8H_8)LaCp''(\mu\text{-}\eta^8\text{:}\eta^8\text{-}C_8H_8)LaCp''_2]$, 4, and $[K(2.2.2\text{-cryptand})][Cp'_2La(\eta^8\text{-}C_8H_8)]^{48}$

| | 4 | $[K(2.2.2\text{-cryptand})][Cp'_2La(\eta^8\text{-}C_8H_8)]^{48}$ |
|------------------------------------------------------|--------------|------------------------------------------------------------------|
| Ln1–Cnt(Cp) | 2.687 | 2.687 |
| | 2.704 | 2.693 |
| Ln2–Cnt(Cp) | 2.547 | |
| Ln1–Cnt(C ₈ H ₈) | 2.190 | 2.159 |
| Ln2–Cnt(C ₈ H ₈) | 2.078 | |
| Ln1–C(Cp) _{avg} | 2.95(5) | 2.95(2) |
| Ln2–C(Cp) _{avg} | 2.81(2) | |
| Ln1–C(C ₈ H ₈) _{avg} | 2.86(4) | 2.83(3) |
| Ln2–C(C ₈ H ₈) _{avg} | ^a | |
| Cnt(Cp)–Ln1–Cnt(Cp) | 109.3 | 107.1 |
| Cnt(Cp)–Ln1–Cnt(C ₈ H ₈) | 125.5 | 126.4 |
| | 125.2 | 126.4 |
| Cnt(Cp)–Ln2–Cnt(C ₈ H ₈) | 117.7 | |

^aNot available due to disorder.

large magnetic anisotropy of the Dy³⁺ and Tb³⁺ ions, enables single-molecule magnet behavior.^{21,22} Magnetic studies on **1** are consistent with a strongly coupled $S = 1/2$ system, with $J_{La-C_6H_6} > 1 - 400 \text{ cm}^{-1}$. This is the first evidence of magnetic exchange coupling in a complex of two nonclassical Ln²⁺ ions bridged by a radical ligand and suggests that this arene Ln–(radical)–Ln moiety could support single-molecule magnet behavior, if suitable magnetically anisotropic lanthanide ions are incorporated, via formation of a strongly exchange-coupled, large total angular momentum ground state.

The greater thermal stability of **1** compared to other La²⁺ complexes is apparent in that **1** does not react with anthracene (−1.74 V vs SHE)⁵⁵ or naphthalene (−2.36 V vs SHE) at room temperature.⁵⁵ The unusual stability of **1** was also demonstrated by Lappert et al., who prepared it at 70 °C.² Compound **1** does react with cyclooctatetraene (−1.59 V vs SHE)⁵⁵ at room temperature, however. In contrast, the four- and one-electron reductants, $[K(2.2.2\text{-cryptand})]_2[(Cp'_2La)_2(C_6H_6)]$ and $[K(2.2.2\text{-cryptand})][Cp'_3La]$, respectively, reduce naphthalene at room temperature.^{20,47} The reactions of **1** with anthracene, naphthalene, and cyclooctatetraene all involve two-electron reductions of the substrate. Since the products are isolated in only 30–60% yield and no other products were identified, it is not possible to know the stoichiometries of these reactions. Hence, although complex **1** can effect two-electron reductions, evidence for stoichiometric three-electron reductions was not available with these substrates.

CONCLUSION

The inverse sandwich reduced arene complex $[K(18\text{-crown}\text{-}6)(THF)_2][(Cp''_2La)_2(\mu\text{-}\eta^6\text{:}\eta^6\text{-}C_6H_6)]$, **1**, originally synthesized by Lappert and co-workers² was definitively identified by X-ray crystallography. The structure of **1**, like its Cp^{tt} analogue, is disordered, precluding a detailed structural analysis, but it was found to contain a planar reduced arene ring surrounded by a planar array of four cyclopentadienyl rings of the two Cp''₂La metallocene units. Magnetic studies of **1** are consistent with an electronic configuration assignment of two 5d¹ La²⁺ ions and a (C₆H₆)¹⁻ radical and demonstrate the first measurement of magnetic exchange coupling between two nontraditional 4f⁰5d¹ Ln²⁺ ions bridged by a radical ligand. The structural characterization of the complexes $[K(18\text{-crown}\text{-}6)(THF)_2][Cp''_2La(\eta^4\text{-}C_{10}H_8)]$, **3**, and $[K(18\text{-crown}\text{-}6)][(\mu\text{-}\eta^8\text{:}\eta^2\text{-}C_8H_8)LaCp''(\mu\text{-}\eta^8\text{:}\eta^8\text{-}C_8H_8)LaCp''_2]$, **4**, demonstrates that the Cp'' ligand is

similar to the Cp' ligand in forming complexes of composition $[Cp''_2Ln(\text{substrate})]^{1-}$. Although **1** can effect two-electron reductions of these substrates, it must be heated to react with substrates that have a reduction potential at or more negative than −1.74 V vs SHE.

ASSOCIATED CONTENT

Supporting Information

The Supporting Information is available free of charge on the ACS Publications website at DOI: [10.1021/acs.organomet.8b00523](https://doi.org/10.1021/acs.organomet.8b00523).

Additional crystallographic information for **3** (CCDC 1857747) and **4** (CCDC 1857746) and magnetic data (PDF)

Accession Codes

CCDC 1857746 and 1857747 contain the supplementary crystallographic data for this paper. These data can be obtained free of charge via www.ccdc.cam.ac.uk/data_request/cif, or by emailing data_request@ccdc.cam.ac.uk, or by contacting The Cambridge Crystallographic Data Centre, 12 Union Road, Cambridge CB2 1EZ, UK; fax: +44 1223 336033.

AUTHOR INFORMATION

Corresponding Authors

*E-mail: wevans@uci.edu (W.J.E.).

*E-mail: jrlong@berkeley.edu (J.R.L.).

ORCID

Chad T. Palumbo: [0000-0001-6436-4602](https://orcid.org/0000-0001-6436-4602)

Megan T. Dumas: [0000-0001-7000-2130](https://orcid.org/0000-0001-7000-2130)

Jeffrey R. Long: [0000-0002-5324-1321](https://orcid.org/0000-0002-5324-1321)

William J. Evans: [0000-0002-0651-418X](https://orcid.org/0000-0002-0651-418X)

Notes

The authors declare no competing financial interest.

ACKNOWLEDGMENTS

We thank the U.S. National Science Foundation for support of this research through grants CHE-1565776 (W.J.E) and CHE-1800252 (J.R.L.). We further thank the NSF Graduate Research Fellowship Program for support of C.T.P. and L.E.D. We thank Jason R. Jones and Mikey Wojnar, for assistance with the X-ray crystallography, and Professor A. S. Borovik for assistance with EPR and UV-vis spectroscopy.

■ REFERENCES

(1) Cassani, M. C.; Gun'ko, Y. K.; Hitchcock, P. B.; Lappert, M. F. The first metal complexes containing the 1,4-cyclohexa-2,5-dienyl ligand (benzene 1,4-dianion); synthesis and structures of $[K(18\text{-crown-6})][Ln\{\eta^5\text{-C}_5\text{H}_3(\text{SiMe}_3)_2\text{-1,3}\}_2(\text{C}_6\text{H}_6)]$ ($Ln = \text{La, Ce}$). *Chem. Commun.* **1996**, 1987–1988.

(2) Cassani, M. C.; Duncalf, D. J.; Lappert, M. F. The First Example of a Crystalline Subvalent Organolanthanum Complex: $[K([18]\text{crown-6})\text{-}(\eta^2\text{-C}_6\text{H}_6)_2][(\text{LaCp}^{\text{tt}})_2(\mu\text{-}\eta^6\text{-C}_6\text{H}_6)]\bullet 2\text{C}_6\text{H}_6$ ($\text{Cp}^{\text{tt}} = \eta^5\text{-C}_5\text{H}_3\text{Bu}^{\text{t-1,3}}$). *J. Am. Chem. Soc.* **1998**, *120*, 12958–12959.

(3) Gun'ko, Y. K.; Hitchcock, P. B.; Lappert, M. F. Nonclassical Organolanthanoid Metal Chemistry: $[K([18]\text{-crown-6})\text{-}(\eta^2\text{-PhMe})_2]X$ ($X = [(\text{LnCp}^{\text{t}})_2(\mu\text{-H})], [(\text{LnCp}^{\text{tt}})_2(\mu\text{-}\eta^6\text{-PhMe})]$) from $[\text{LnCp}^{\text{t}}_3]$, K , and $[18]\text{-crown-6}$ in Toluene ($Ln = \text{La, Ce}$; $\text{Cp}^{\text{t}} = \eta^5\text{-C}_5\text{H}_4\text{SiMe}_2\text{Bu}^{\text{t}}$; $\text{Cp}^{\text{tt}} = \eta^5\text{-C}_5\text{H}_3(\text{SiMe}_3)_2\text{-1,3}$). *Organometallics* **2000**, *19*, 2832–2834.

(4) Hitchcock, P. B.; Lappert, M. F.; Maron, L.; Protschenko, A. V. Lanthanum Does Form Stable Molecular Compounds in the +2 Oxidation State. *Angew. Chem., Int. Ed.* **2008**, *47*, 1488–1491.

(5) Fryzuk, M. D.; Love, J. B.; Rettig, S. J. Arene Coordination to Yttrium(III) via Carbon–Carbon Bond Formation. *J. Am. Chem. Soc.* **1997**, *119*, 9071–9072.

(6) Fryzuk, M. D.; Jafarpour, L.; Kerton, F. M.; Love, J. B.; Patrick, B. O.; Rettig, S. J. Carbon–Carbon Bond Formation Using Yttrium(III) and the Lanthanide Elements. *Organometallics* **2001**, *20*, 1387–1396.

(7) Bochkarev, M. N. Synthesis, Arrangement, and Reactivity of Arene–Lanthanide Compounds. *Chem. Rev.* **2002**, *102*, 2089–2118.

(8) Huang, W.; Dulong, F.; Wu, T.; Khan, S. I.; Miller, J. T.; Cantat, T.; Diaconescu, P. L. A six-carbon 10 π -electron aromatic system supported by group 3 metals. *Nat. Commun.* **2013**, *4*, 1448.

(9) Diaconescu, P. L.; Arnold, P. L.; Baker, T. A.; Mindiola, D. J.; Cummins, C. C. Arene-Bridged Diuranium Complexes: Inverted Sandwiches Supported by δ Backbonding. *J. Am. Chem. Soc.* **2000**, *122*, 6108–6109.

(10) Evans, W. J.; Kozimor, S. A.; Ziller, J. W.; Kaltsoyannis, N. Structure, Reactivity, and Density Functional Theory Analysis of the Six-Electron Reductant, $[(\text{C}_5\text{Me}_5)_2\text{U}]_2(\mu\text{-}\eta^6\text{-C}_6\text{H}_6)$, Synthesized via a New Mode of $(\text{C}_5\text{Me}_5)_3\text{M}$ Reactivity. *J. Am. Chem. Soc.* **2004**, *126*, 14533–14547.

(11) Arnold, P. L.; Mansell, S. M.; Maron, L.; McKay, D. Spontaneous reduction and C–H borylation of arenes mediated by uranium(III) disproportionation. *Nat. Chem.* **2012**, *4*, 668–674.

(12) Patel, D.; Tuna, F.; McInnes, E. J.; McMaster, J.; Lewis, W.; Blake, A. J.; Liddle, S. T. A triamido-uranium(V) inverse-sandwich 10-toluene tetraanion arene complex. *Dalton Trans.* **2013**, *42*, 5224–5227.

(13) Camp, C.; Mougel, V.; Pecaut, J.; Maron, L.; Mazzanti, M. Cation-Mediated Conversion of the State of Charge in Uranium Arene Inverted-Sandwich Complexes. *Chem. - Eur. J.* **2013**, *19*, 17528–17540.

(14) MacDonald, M. R.; Ziller, J. W.; Evans, W. J. Synthesis of a Crystalline Molecular Complex of Y^{2+} , $[(18\text{-crown-6})\text{K}]_2[(\text{C}_5\text{H}_4\text{-SiMe}_3)_3\text{Y}]$. *J. Am. Chem. Soc.* **2011**, *133*, 15914–15917.

(15) MacDonald, M. R.; Bates, J. E.; Fieser, M. E.; Ziller, J. W.; Furche, F.; Evans, W. J. Expanding Rare-Earth Oxidation State Chemistry to Molecular Complexes of Holmium(II) and Erbium(II). *J. Am. Chem. Soc.* **2012**, *134*, 8420–8423.

(16) MacDonald, M. R.; Bates, J. E.; Ziller, J. W.; Furche, F.; Evans, W. J. Completing the Series of +2 Ions for the Lanthanide Elements: Synthesis of Molecular Complexes of Pr^{2+} , Gd^{2+} , Tb^{2+} , and Lu^{2+} . *J. Am. Chem. Soc.* **2013**, *135*, 9857–9868.

(17) Fieser, M. E.; MacDonald, M. R.; Krull, B. T.; Bates, J. E.; Ziller, J. W.; Furche, F.; Evans, W. J. Structural, Spectroscopic, and Theoretical Comparison of Traditional vs Recently Discovered Ln^{2+} Ions in the $[\text{K}(2.2.2\text{-cryptand})][(\text{C}_5\text{H}_4\text{-SiMe}_3)_3\text{Ln}]$ Complexes: The Variable Nature of Dy^{2+} and Nd^{2+} . *J. Am. Chem. Soc.* **2015**, *137*, 369–382.

(18) Evans, W. J. Tutorial on the Role of Cyclopentadienyl Ligands in the Discovery of Molecular Complexes of the Rare-Earth and Actinide Metals in New Oxidation States. *Organometallics* **2016**, *35*, 3088–3100.

(19) Woen, D. H.; Evans, W. J. In *Handbook on the Physics and Chemistry of Rare Earths*, 1st ed.; Elsevier: Amsterdam, 2016; Vol. 50, pp 337–394.

(20) Kotyk, C. M.; Fieser, M. E.; Palumbo, C. T.; Ziller, J. W.; Darago, L. E.; Long, J. R.; Furche, F.; Evans, W. J. Isolation of +2 rare earth metal ions with three anionic carbocyclic rings: bimetallic bis(cyclopentadienyl) reduced arene complexes of La^{2+} and Ce^{2+} are four electron reductants. *Chem. Sci.* **2015**, *6*, 7267–7273.

(21) Rinehart, J. D.; Fang, M.; Evans, W. J.; Long, J. R. Strong exchange and magnetic blocking in N_2^{3-} -radical-bridged lanthanide complexes. *Nat. Chem.* **2011**, *3*, 538–542.

(22) Rinehart, J. D.; Fang, M.; Evans, W. J.; Long, J. R. A N_2^{3-} Radical-Bridged Terbium Complex Exhibiting Magnetic Hysteresis at 14 K. *J. Am. Chem. Soc.* **2011**, *133*, 14236–14239.

(23) Demir, S.; Zadrozny, J. M.; Nippe, M.; Long, J. R. Exchange Coupling and Magnetic Blocking in Bipyrimidyl Radical-Bridged Dilanthanide Complexes. *J. Am. Chem. Soc.* **2012**, *134*, 18546–18549.

(24) Demir, S.; Nippe, M.; Gonzalez, M. I.; Long, J. R. Exchange coupling and magnetic blocking in dilanthanide complexes bridged by the multi-electron redox-active ligand 2,3,5,6-tetra(2-pyridyl)pyrazine. *Chem. Sci.* **2014**, *5*, 4701–4711.

(25) Demir, S.; Jeon, I. R.; Long, J. R.; Harris, T. D. Radical ligand-containing single-molecule magnets. *Coord. Chem. Rev.* **2015**, *289*–290, 149–176.

(26) Dolinar, B. S.; Gomez-Coca, S.; Alexandropoulos, D. I.; Dunbar, K. R. An air stable radical-bridged dysprosium single molecule magnet and its neutral counterpart: redox switching of magnetic relaxation dynamics. *Chem. Commun.* **2017**, *53*, 2283–2286.

(27) Gould, C. A.; Darago, L. E.; Gonzalez, M. I.; Demir, S.; Long, J. R. A Trinuclear Radical-Bridged Lanthanide Single-Molecule Magnet. *Angew. Chem., Int. Ed.* **2017**, *56*, 10103–10107.

(28) Guo, F. S.; Layfield, R. A. Strong direct exchange coupling and single-molecule magnetism in indigo-bridged lanthanide dimers. *Chem. Commun.* **2017**, *53*, 3130–3133.

(29) Evans, W. J.; Fang, M.; Zucchi, G.; Furche, F.; Ziller, J. W.; Hoekstra, R. M.; Zink, J. I. Isolation of Dysprosium and Yttrium Complexes of a Three-Electron Reduction Product in the Activation of Dinitrogen, the $(\text{N}_2)^{3-}$ Radical. *J. Am. Chem. Soc.* **2009**, *131*, 11195–11202.

(30) Meihaus, M. R.; Corbey, J. F.; Fang, M.; Ziller, J. W.; Long, J. R.; Evans, W. J. Influence of an Inner-Sphere K^+ Ion on the Magnetic Behavior of N_2^{3-} Radical-Bridged Dilanthanide Complexes Isolated Using an External Magnetic Field. *Inorg. Chem.* **2014**, *53*, 3099–3107.

(31) Demir, S.; Gonzalez, M. I.; Darago, L. E.; Evans, W. J.; Long, J. R. Giant coercivity and high magnetic blocking temperatures for N_2^{3-} radical-bridged dilanthanide complexes upon ligand dissociation. *Nat. Commun.* **2017**, *8*, 2144.

(32) Xie, Z.; Chui, K.; Liu, Z.; Xue, F.; Zhang, Z.; Mak, T. C. W.; Sun, J. Systematic studies on the reactions of lanthanide trichlorides with $\text{Na}[1,3\text{-bis(trimethylsilyl)cyclopentadienyl}]$. Crystal structures of $[1,3\text{-}(\text{Me}_3\text{Si})_2\text{C}_5\text{H}_3]_3\text{Ln}$ ($Ln = \text{La, Nd, Gd, Dy}$). *J. Organomet. Chem.* **1997**, *549*, 239–244.

(33) Rabe, G. W.; Ziller, J. W. Phosphido Complexes of the Lanthanides. Synthesis and x-ray Crystal Structure Determination of a Tris(phosphido) Species of Neodymium: $\text{Nd}[\text{P}(\text{SiMe}_3)_3]_3(\text{thf})_2$. *Inorg. Chem.* **1995**, *34*, 5378–5379.

(34) Langeslay, R. R.; Fieser, M. E.; Ziller, J. W.; Furche, F.; Evans, W. J. Expanding Thorium Hydride Chemistry Through Th^{2+} , Including the Synthesis of a Mixed-Valent $\text{Th}^{4+}/\text{Th}^{3+}$ Hydride Complex. *J. Am. Chem. Soc.* **2016**, *138*, 4036–4045.

(35) Fieser, M. E.; Palumbo, C. T.; La Pierre, H. S.; Halter, D. P.; Voora, V. K.; Ziller, J. W.; Furche, F.; Meyer, K.; Evans, W. J. Comparisons of lanthanide/actinide +2 ions in a tris(aryloxide)arene coordination environment. *Chem. Sci.* **2017**, *8*, 7424–7433.

(36) Windorff, C. J.; MacDonald, M. R.; Meihaus, M. R.; Ziller, J. W.; Long, J. R.; Evans, W. J. Expanding the Chemistry of Molecular U^{2+} Complexes: Synthesis, Characterization, and Reactivity of the $[(\text{C}_5\text{H}_3\text{-SiMe}_3)_2\text{U}]^-$ Anion. *Chem. - Eur. J.* **2016**, *22*, 772–782.

(37) Woen, D. H.; Chen, G. P.; Ziller, J. W.; Boyle, T. J.; Furche, F.; Evans, W. J. Solution Synthesis, Structure, and CO_2 Reduction Reactivity of a Scandium(II) Complex, $\{\text{Sc}[\text{N}(\text{SiMe}_3)_2]_3\}^-$. *Angew. Chem., Int. Ed.* **2017**, *56*, 2050–2053.

(38) Bain, G. A.; Berry, J. F. Diamagnetic Corrections and Pascal's Constants. *J. Chem. Educ.* **2008**, *85*, 532–536.

(39) Chilton, N. F.; Anderson, R. P.; Turner, L. D.; Soncini, A.; Murray, K. S. PHI: a powerful new program for the analysis of anisotropic monomeric and exchange-coupled polynuclear d- and f-block complexes. *J. Comput. Chem.* **2013**, *34*, 1164–1175.

(40) Hu, Z.; Dong, B. W.; Liu, Z.; Liu, J. J.; Su, J.; Yu, C.; Xiong, J.; Shi, D. E.; Wang, Y.; Wang, B. W.; Ardavan, A.; Shi, Z.; Jiang, S. D.; Gao, S. Endohedral Metallofullerene as Molecular High Spin Qubit: Diverse Rabi Cycles in $\text{Gd}_2@\text{C}_{79}\text{N}$. *J. Am. Chem. Soc.* **2018**, *140*, 1123–1130.

(41) Van Vleck, J. H. Paramagnetic Relaxation and the Equilibrium of Lattice Oscillators. *Phys. Rev.* **1941**, *59*, 724–729.

(42) Chiorescu, I.; Wernsdorfer, W.; Müller, A.; Böggel, H.; Barbara, B. Butterfly Hysteresis Loop and Dissipative Spin Reversal in the $S = 1/2$, V_{15} Molecular Complex. *Phys. Rev. Lett.* **2000**, *84*, 3454–3457.

(43) Tesi, L.; Lunghi, A.; Atzori, M.; Lucaccini, E.; Sorace, L.; Totti, F.; Sessoli, R. Giant spin–phonon bottleneck effects in evaporable vanadyl-based molecules with long spin coherence. *Dalton Trans.* **2016**, *45*, 16635–16645.

(44) Huang, W.; Khan, S. I.; Diaconescu, P. L. Scandium Arene Inverted-Sandwich Complexes Supported by a Ferrocene Diamide Ligand. *J. Am. Chem. Soc.* **2011**, *133*, 10410–10413.

(45) Huang, W.; Abukhalil, P. M.; Khan, S. I.; Diaconescu, P. L. Group 3 metal stilbene complexes: synthesis, reactivity, and electronic structure studies. *Chem. Commun.* **2014**, *50*, 5221–5223.

(46) Fryzuk, M. D.; Jafarpour, L.; Kerton, F. M.; Love, J. B.; Rettig, S. J. Dinuclear π Complexes of Yttrium and Lutetium with Sandwiched Naphthalene and Anthracene Ligands: Evidence for Rapid Intramolecular Inter-Ring Rearrangements. *Angew. Chem., Int. Ed.* **2000**, *39*, 767–770.

(47) Kotyk, C. M.; MacDonald, M. R.; Ziller, J. W.; Evans, W. J. Reactivity of the Ln^{2+} Complexes $[\text{K}(2.2.2\text{-cryptand})][(\text{C}_5\text{H}_4\text{SiMe}_3)_3\text{Ln}]$: Reduction of Naphthalene and Biphenyl. *Organometallics* **2015**, *34*, 2287–2295.

(48) Palumbo, C. T.; Fieser, M. E.; Ziller, J. W.; Evans, W. J. Reactivity of Complexes of $4f^55d^1$ and $4f^{n+1}\text{Ln}^{2+}$ Ions with Cyclooctatetraene. *Organometallics* **2017**, *36*, 3721–3728.

(49) Hazin, P. N.; Bruno, J. W.; Schulte, G. K. Syntheses of organolanthanum and -cerium cations and labile precursors. *Organometallics* **1990**, *9*, 416–423.

(50) Evans, W. J.; Mueller, T. J.; Ziller, J. W. Reactivity of $(\text{C}_5\text{Me}_5)_3\text{LaL}_x$ Complexes: Synthesis of a Tris(pentamethylcyclopentadienyl) Complex with Two Additional Ligands, $(\text{C}_5\text{Me}_5)_3\text{La}(\text{NCCMe}_3)_2$. *J. Am. Chem. Soc.* **2009**, *131*, 2678–2686.

(51) Hamaed, H.; Lo, A. Y.; Lee, D. S.; Evans, W. J.; Schurko, R. W. Solid-State ^{139}La and ^{15}N NMR Spectroscopy of Lanthanum-Containing Metallocenes. *J. Am. Chem. Soc.* **2006**, *128*, 12638–12639.

(52) Meihaus, M. R.; Fieser, M. E.; Corbey, J. F.; Evans, W. J.; Long, J. R. Record High Single-Ion Magnetic Moments Through $4f^75d^1$ Electron Configurations in the Divalent Lanthanide Complexes $[(\text{C}_5\text{H}_4\text{SiMe}_3)_3\text{Ln}]^-$. *J. Am. Chem. Soc.* **2015**, *137*, 9855–9860.

(53) Fang, M.; Bates, J. E.; Lorenz, S. E.; Lee, D. S.; Rego, D. B.; Ziller, J. W.; Furche, F.; Evans, W. J. $(\text{N}_2)^{3-}$ Radical Chemistry via Trivalent Lanthanide Salt/Alkali Metal Reduction of Dinitrogen: New Syntheses and Examples of $(\text{N}_2)^{2-}$ and $(\text{N}_2)^{3-}$ Complexes and Density Functional Theory Comparisons of Closed Shell Sc^{3+} , Y^{3+} , and Lu^{3+} versus $4f^9\text{Dy}^{3+}$. *Inorg. Chem.* **2011**, *50*, 1459–1469.

(54) Fang, M.; Lee, D. S.; Ziller, J. W.; Doedens, R. J.; Bates, J. E.; Furche, F.; Evans, W. J. Synthesis of the $(\text{N}_2)^{3-}$ Radical from Y^{2+} and Its Protonolysis Reactivity To Form $(\text{N}_2\text{H}_2)^{2-}$ via the $\text{Y}[\text{N}(\text{SiMe}_3)_2]_3/\text{KC}_8$ Reduction System. *J. Am. Chem. Soc.* **2011**, *133*, 3784–3787.

(55) Evans, W. J.; Gonzales, S. L.; Ziller, J. W. Reactivity of Decamethylsamarocene with Polycyclic Aromatic Hydrocarbons. *J. Am. Chem. Soc.* **1994**, *116*, 2600–2608.